DITEN

U.R.S.I.
Italian National Committee

2023 Italian National URSI meeting
November 17, 2023
Genova

2023 | GENOA IEEE CAMA

Microwave Imaging Techniques and Applications

(in memory of Matteo Pastorino)

Andrea Randazzo and Alessandro Fedeli

AEM Applied Electromagnetics Group

University of Genoa
Department of Electrical, Electronic, Telecommunications Engineering and Naval Architecture (DITEN)

In memoriam – Prof. Matteo Pastorino

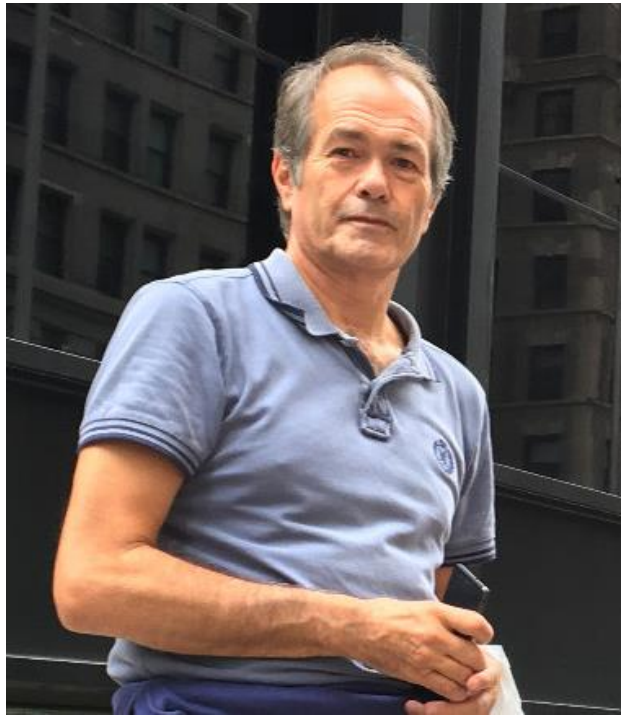

Matteo Pastorino (IEEE Fellow) passed away on 5 June 2023 at the age of 61:

- Full professor of electromagnetic fields at the University of Genoa, Italy
- Department's Director several times (DIBE 2008-2011, DITEN 2012-2014 and 2018-2021)
- Vice Rector for Technology Transfer (2021-2022)

He was a very prolific and brilliant scientist in the field of applied electromagnetics:

- Co-authors of more than 600 papers in international journals and conferences.
- Author of the book Microwave Imaging (Wiley, 2010) and co-author the book Microwave Imaging Methods and Applications (Artech House, 2018).

His research interests ranged among several aspects of applied electromagnetics:

- Electromagnetic imaging and diagnostic systems (he was one of the pioneers in this topic, starting his work in the field in the eighties of the previous century)
- Antennas and propagation
- Analytical and numerical techniques for direct and inverse electromagnetic scattering

In memoriam – Prof. Matteo Pastorino

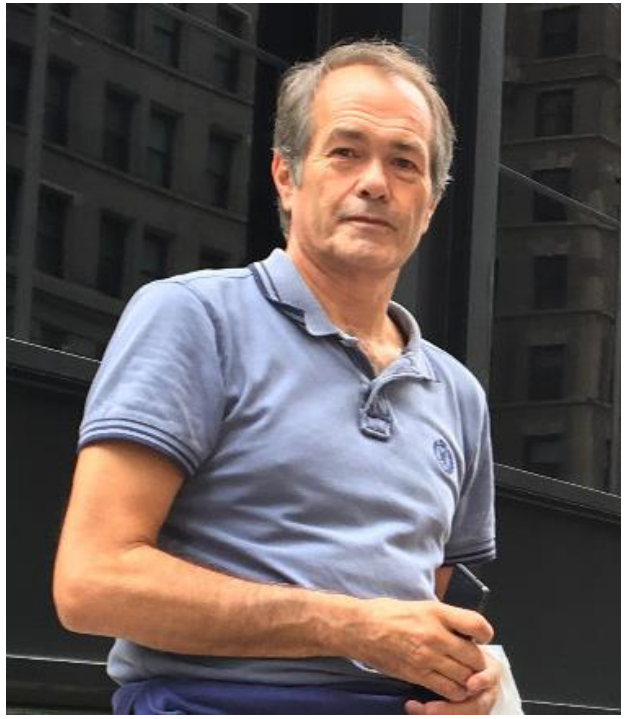

Prof. Pastorino was involved in the IEEE and URSI with a high level of commitment:

- Member of the Administrative Committee (AdCom) of IEEE IMS (2007-2010)
- Member of the URSI Commission B Technical Advisory Board (from 2017).
- Officer (chair) of the Commission B of the Italian CNR-URSI Commission (2014-2022).

He was nominated IEEE Fellow in 2009 "For the contributions in the analysis of electromagnetic scattering".

He has been chair of different IEEE conferences

- General Chair of the 2023 IEEE CAMA
- Honorary co-chair of the IEEE International Conference on Imaging Systems and Techniques since its establishment.

In addition to his great scientific accomplishments, he was primarily a wonderful person, beloved among all his relatives, colleagues, and students. His kind, humble and sympathetic character, together with his tenacity, enthusiasm, and sensitivity to others' needs, made him an extraordinary example.

In memoriam – Prof. Matteo Pastorino

Microwave imaging
(Wiley, 2010)

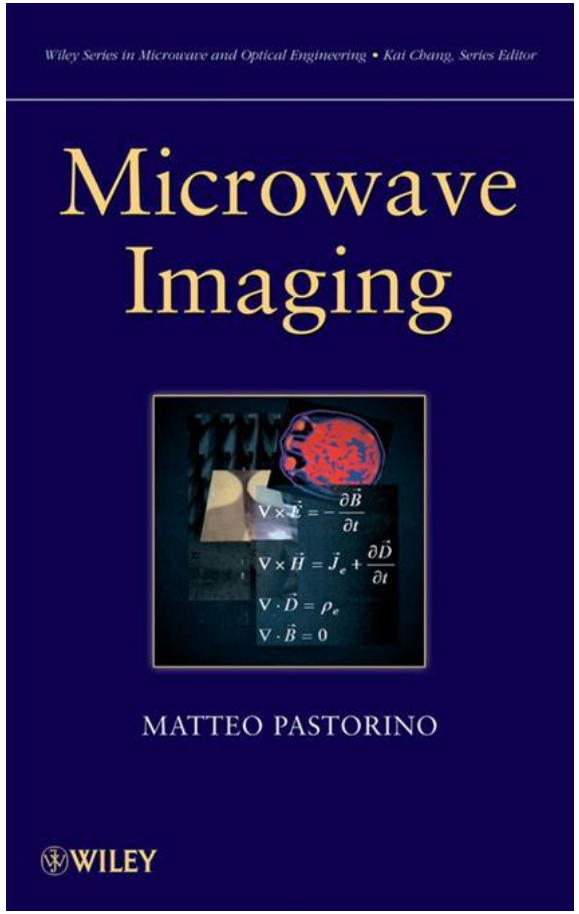

Microwave imaging Methods and Application
(Artech House, 2018)

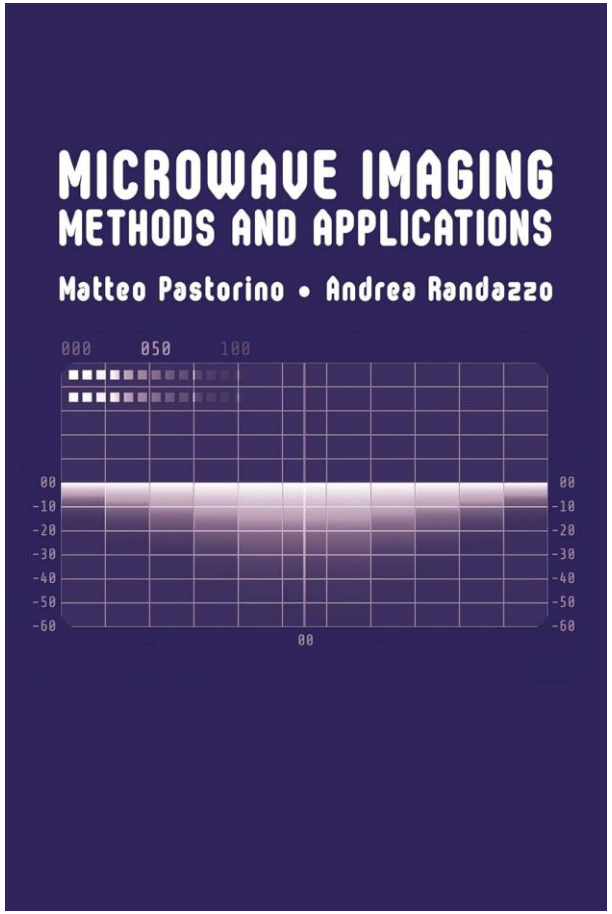

Microwave Imaging based on Inverse Scattering: Techniques, Systems and Applications
(Texmat, 2023)

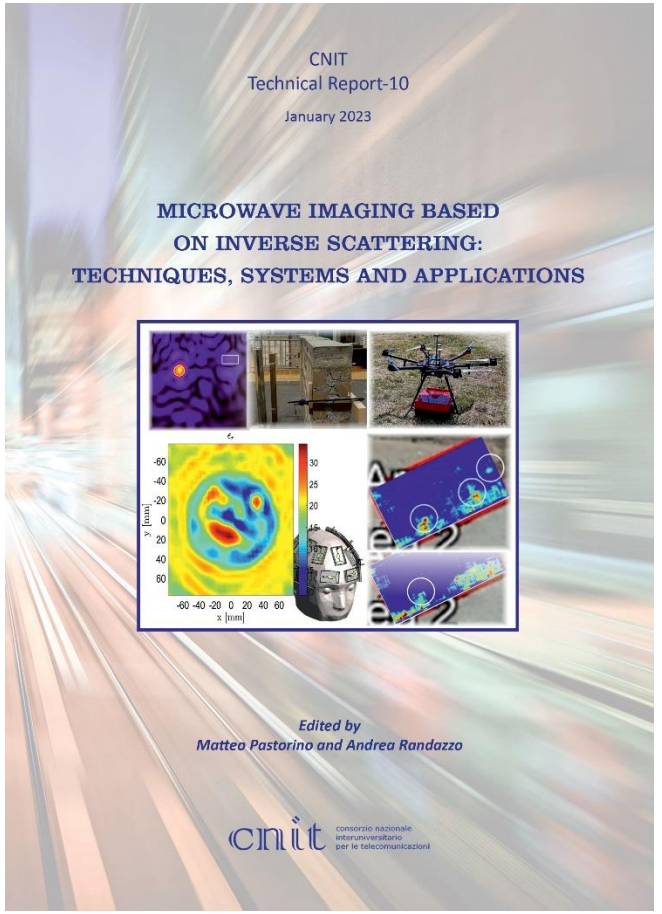

Introduction to Microwave Imaging

- **Microwave imaging:** Noninvasive and nondestructive techniques aimed at sensing materials or targets in order to retrieve some physical properties, and/or to deduce information about the conditions of the structures under test [1][2].
- Common approaches:
  - Radar-based imaging
  - Microwave holography
  - …
  - **Inverse scattering-based imaging**

The talk will be focused on this class of approaches

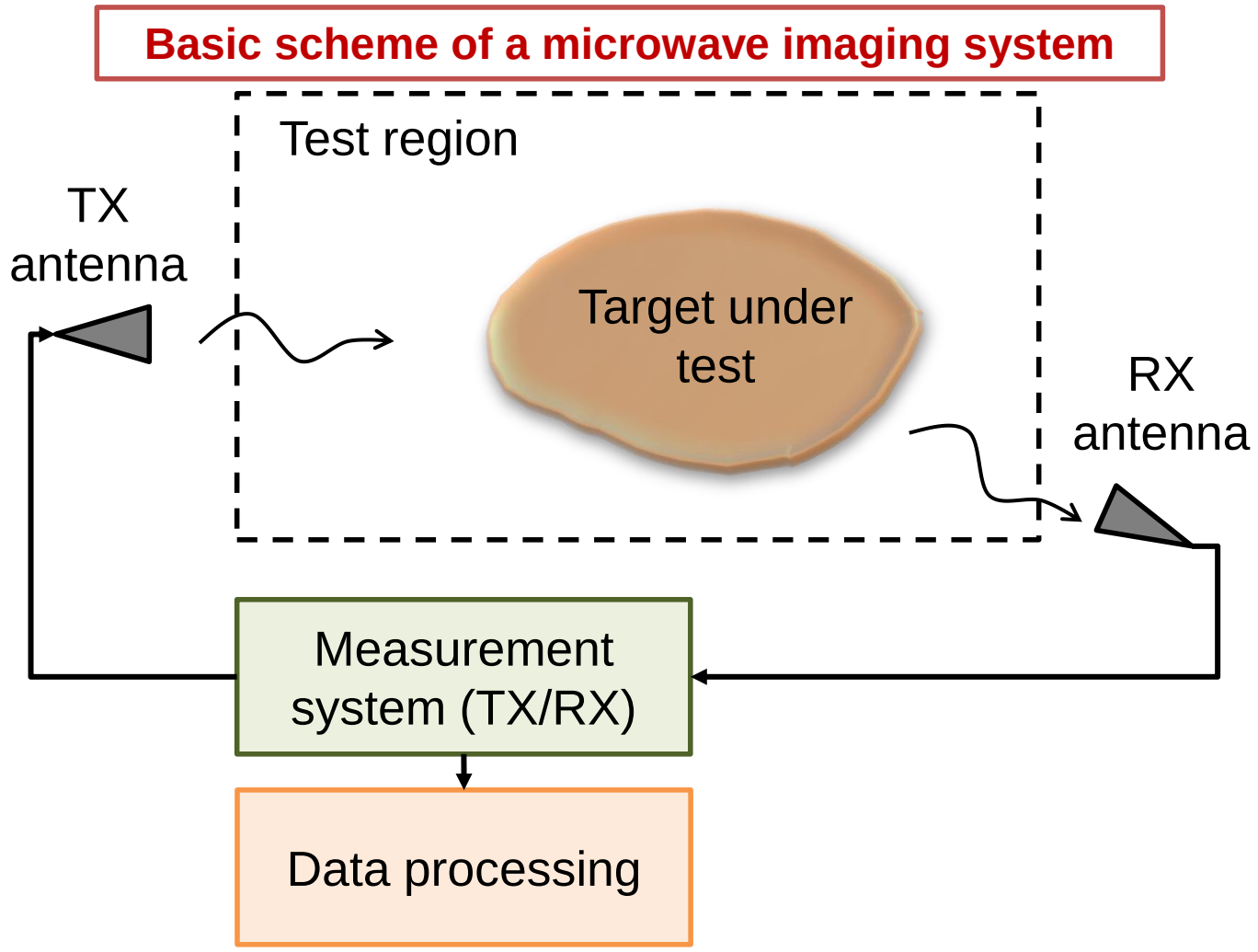

[1] M. Pastorino, **Microwave Imaging**, Wiley, 2010.
[2] M. Pastorino and A. Randazzo, **Microwave imaging Methods and Application**, Boston, MA: Artech House, 2018.

Electromagnetic inverse scattering basics (dielectric targets)

- The targets are located in a volume V_{inv}, characterized by a complex dielectric permittivity $\epsilon(\mathbf{r}), = \epsilon_0\epsilon_r(\mathbf{r}) - j\sigma(\mathbf{r})/\omega$.
- Background medium has complex dielectric permittivity ϵ_b.
- The investigation volume is illuminated by one or more incident electric fields $\mathbf{E}_{inc}(\mathbf{r})$ (generated by one or more TX antennas).
- The electric field $\mathbf{E}_{tot}(\mathbf{r})$, resulting from the interaction between the target and the illuminating radiation, is collected by means of RX antennas located in a known measurement domain D_{obs}.

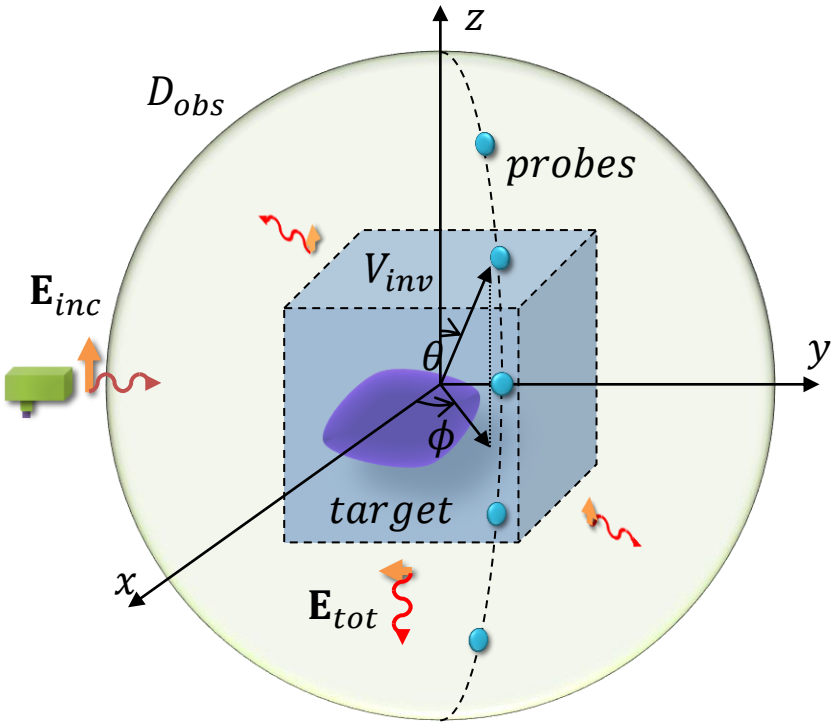

- Basic equation governing EM scattering:

Dielectric contrast: $c = \frac{\epsilon}{\epsilon_b} - 1$

$$\mathbf{E}_{tot}(\mathbf{r}) = \mathbf{E}_{inc}(\mathbf{r}) + \mathbf{E}_{scat}(\mathbf{r}) = \mathbf{E}_{inc}(\mathbf{r}) - k_b^2 \int_{V_{inv}} c(\mathbf{r}')\mathbf{E}_{tot}(\mathbf{r}') \cdot \bar{\mathbf{G}}_b(\mathbf{r}, \mathbf{r}')d\mathbf{r}'$$

Dyadic Green's function

Electromagnetic inverse scattering basics (dielectric targets)

- The previous equation can be used to relate the data (measured total field) to the unknown (dielectric properties) → data equation
- However, the total field inside the target is unknown → A second equation is needed (state equation).

Scattered electric field ($\mathbf{E}_{scatt}^{meas} = \mathbf{E}_{tot}^{meas} - \mathbf{E}_{inc}^{meas}$)

$$\begin{cases} \mathbf{E}_{scatt}^{meas}(\mathbf{r}) = -k_b^2 \int_{V_{inv}} c(\mathbf{r}')\mathbf{E}_{tot}^{int}(\mathbf{r}') \cdot \bar{\mathbf{G}}_b(\mathbf{r},\mathbf{r}')d\mathbf{r}', & \mathbf{r} \in D_{obs} \\ \mathbf{E}_{inc}(\mathbf{r}) = \mathbf{E}_{tot}^{int}(\mathbf{r}) + k_b^2 \int_{V_{inv}} c(\mathbf{r}')\mathbf{E}_{tot}^{int}(\mathbf{r}') \cdot \bar{\mathbf{G}}_b(\mathbf{r},\mathbf{r}')d\mathbf{r}', & \mathbf{r} \in V_{inv} \end{cases}$$

In compact mathematical form…

$$\mathbf{E}_{scatt}^{meas}(\mathbf{r}) = \mathcal{F}(c)(\mathbf{r}), \qquad \mathbf{r} \in D_{obs}$$

3D VECTOR NONLINEAR SCATTERING OPERATOR

Electromagnetic inverse scattering basics (dielectric targets)

- In several cases, the targets may be assumed of cylindrical shape (at least approximately), i.e.,

$$c(\mathbf{r}) = c(x, y)$$

- The target cross section D_{obj} is contained in a known planar domain D_{inv}.
- Moreover, the incident radiation is assumed to be transverse magnetic (TM) with respect to the axial direction z, i.e.,

$$\mathbf{E}_{inc}(\mathbf{r}) = E_{inc}(x, y)\hat{\mathbf{z}}$$

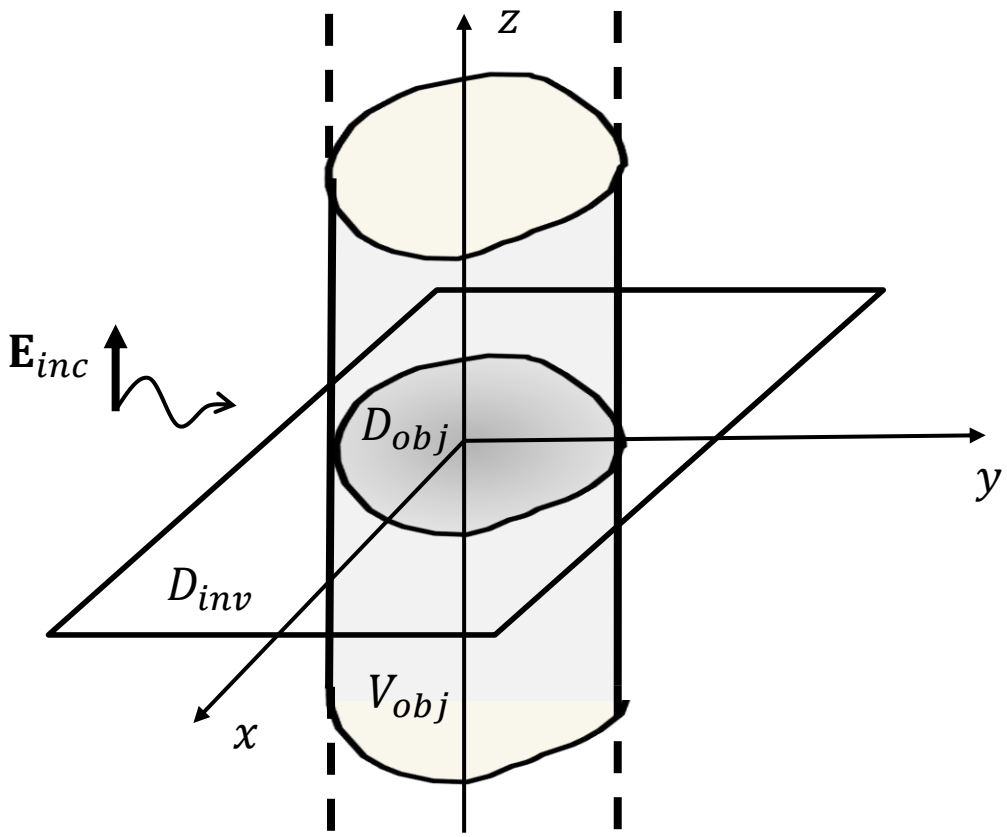

Electromagnetic inverse scattering basics (dielectric targets)

- Under such hypothesis, the scattering problem is described by 2D scalar equations.
- For the 2D problem the fundamental electric field integral equations (EFIEs) become

$$\begin{cases} E_{scatt}^{meas}(x,y) = -k_b^2 \int_{D_{inv}} c(x',y') E_{tot}^{int}(x',y') g_b(x,y,x',y') dx'dy' \,, (x,y) \in D_{obs} \\ E_{inc}(x,y) = E_{tot}^{int}(x,y) + k_b^2 \int_{D_{inv}} c(x',y') E_{tot}^{int}(x',y') g_b(x,y,x',y') dx'dy' \,, (x,y) \in D_{inv} \end{cases}$$

2D scalar Green's function

In compact mathematical form…

$$E_{scatt}^{meas}(x,y) = \mathcal{F}(c)(x,y), (x,y) \in D_{obs}$$

2D SCALAR NONLINEAR SCATTERING OPERATOR

Electromagnetic inverse scattering basics (dielectric targets)

- Other equivalent representations can be used.
- By defining the contrast source current density $J_{cs}(\mathbf{r}) = c(\mathbf{r})E_{tot}(\mathbf{r}),\ \mathbf{r} \in D_{inv}$, the scattering equation become

$$\begin{cases} E_{scatt}^{meas}(x,y) = -k_b^2 \int_{D_{inv}} J_{cs}(x',y') g_b(x,y,x',y') dx'dy' \,, (x,y) \in D_{obs} \\ J_{cs}(x,y) = c(x,y)E_{inc}(x,y) - k_b^2 c(x,y) \int_{D_{inv}} J_{cs}(x',y') g_b(x,y,x',y') dx'dy' \,, (x,y) \in D_{inv} \end{cases}$$

- Advantage: the data equation turns out to be linear → Several methods relies upon such formulation (e.g., the contrast source inversion method).
- Other possible rewrite of the scattering equation has also been recently proposed [2][3].

[1] P. M. van den Berg and R. E. Kleinman, "A contrast source inversion method," ***Inv. Probl.***, 1997.
[2] Y. Zhong, M. Lambert, D. Lesselier, and X. Chen, 'A new integral equation method to solve highly nonlinear inverse scattering problems', ***IEEE Trans. Antennas Propag.***, 2016.
[3] M. D'Urso, T. Isernia, and A. F. Morabito, "On the solution of 2-D inverse scattering problems via source-type integral equation," ***IEEE Trans. Geosci. Remote Sens.***, 2010.

Electromagnetic inverse scattering basics (dielectric targets)

- Most imaging algorithms assume that direct measurements of the electric field are available.
- In practice, S-parameter measurements are available → A different data equation can be exploited:

Scattered S-parameters
$\tilde{S}_{ij}^{sc} = \tilde{S}_{ij}^{tot} - \tilde{S}_{ij}^{inc}$ measured between ports i and j

$$\tilde{S}_{ij}^{sc} = -\frac{j\omega\epsilon_b}{2b_i b_j}\iint_{D_{inv}} E_{inc,i}^{int}(x',y')\,c(x',y')\,E_{tot,j}^{int}(x',y')\,dx'dy'$$

b_m: amplitude of the incident power wave at the mth port

z-components of incident and total electric fields when the ith and the jth antennas are transmitting

[1] N. K. Nikolova, ***Introduction to Microwave Imaging***. Cambridge: Cambridge University Press, 2017.

Electromagnetic inverse scattering problem

- **Objective of the microwave imaging problem**: starting from the measured samples, find an approximation of some model parameters describing the electromagnetic properties of the investigated area (e.g., the distribution of the dielectric permittivity ϵ_r)

- In a mathematical form: given a data function y (the electric field or S-parameters), find an approximation of the unknown function x (e.g., the dielectric contrast) such that

$$\mathcal{F}(x) = y$$

- being $\mathcal{F}$ a nonlinear operator describing the scattering phenomena, $x \in X$ with X space of unknowns, and $y \in Y$ with Y space of data.

Imaging Methods

- **Key problems** associated to the solution of this equation:
  - **Nonlinear** equation with **two unknowns** (the total electric field and the contrast function).
  - Very **ill-posed** inverse problem (Fredholm equation of the first kind)
- The various proposed imaging techniques can be categorized in several ways:
  - Classification based on the dimensionality of the problem (one-, two-, and three-dimensional reconstructions).
  - Classification based on the objective of the inspection and includes qualitative and quantitative methods.

Inverse-scattering methods

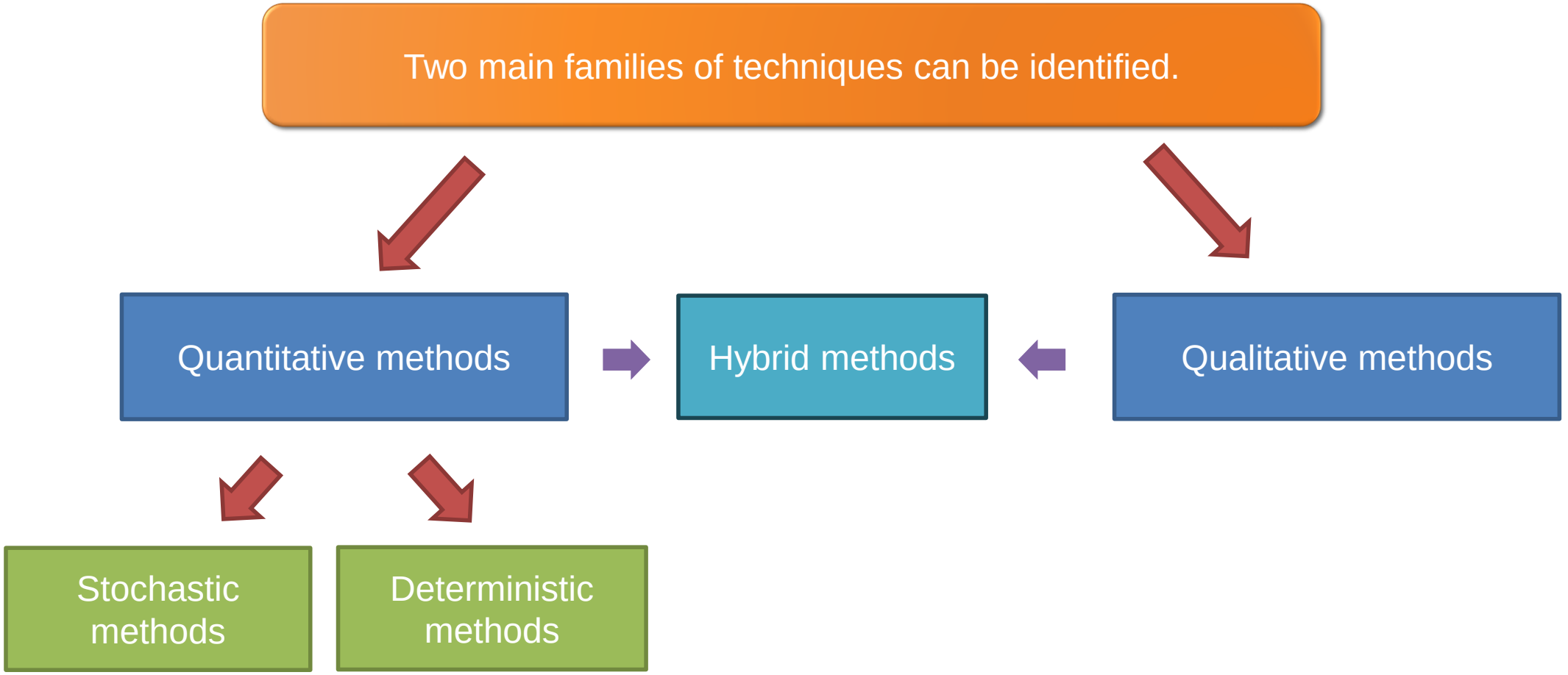

Qualitative Inverse Scattering Methods

- Qualitative methods basically includes two types of approaches:
  - methods aimed at retrieving only some specific information about the target under test (e.g., location, support, shape, presence of interfaces, etc.)
  - methods based on specific approximations on the electromagnetic model (e.g., Born or Rytov ones)

- Some examples of qualitative methods:
  - Linear Sampling Method (LSM) [1]
  - Orthogonality sampling method (OSM) [2]
  - Level Set Method [3]
  - Approaches based on the Born or Rytov approximation, e.g., relying on the use of the truncated singular value decomposition (SVD) inversion technique [4]
  - Subspace methods (MUSIC [5], TSOM [6], …)
  - Beamforming techniques [7]
  - Compressive sensing techniques [8]

[1] L. Crocco, L. Di Donato, I. Catapano, and T. Isernia, 'An improved simple method for imaging the shape of complex targets', ***IEEE Trans. Antennas Propag.***, 2013.
[2] M. T. Bevacqua, T. Isernia, R. Palmeri, M. N. Akinci, and L. Crocco, "Physical insight unveils new imaging capabilities of orthogonality sampling method," ***IEEE Trans. Antennas Propag.***, 2020.
[3] P. Shah and M. Moghaddam, 'A fast level set method for multimaterial recovery in microwave imaging', ***IEEE Trans. Antennas Propag.***, 2018.
[4] D. S. Shumakov and N. K. Nikolova, 'Fast quantitative microwave imaging with scattered-power maps', ***IEEE Trans. Microw. Theory Techn.***, 2018.
[5] R. Solimene and G. Leone, 'MUSIC algorithms for grid diagnostics', ***IEEE Geosci. Remote Sens. Lett.***, 2013.
[6] . Zhong, M. Lambert, D. Lesselier, and X. Chen, 'A new integral equation method to solve highly nonlinear inverse scattering problems', ***IEEE Trans. Antennas Propag.***, 2016
[7] E. C. Fear, X. Li, S. C. Hagness, and M. A. Stuchly, 'Confocal microwave imaging for breast cancer detection: localization of tumors in three dimensions', ***IEEE Trans. Biomed. Eng.***, 2002.
[8] G. Oliveri, L. Poli, N. Anselmi, M. Salucci, and A. Massa, 'Compressive sensing-based born iterative method for tomographic imaging', **IEEE Trans. Microw. Theory Techn.**, 2019.

Quantitative Inverse Scattering Methods

- Quantitative methods are aimed at retrieving the full distributions of the dielectric parameters of the target, by solving the inverse scattering problem in its full non-linear form.
- **Stochastic methods** → potentially able to find the global minima, but usually requiring high computational resources [1]-[4]
  - Genetic algorithm
  - Differential evolution
  - Particle swarm optimization
  - Artificial bee colony
- **Deterministic methods** → usually fast, but may be trapped in local minima [5]-[9]
  - Contrast source inversion
  - Newton-based schemes
  - Gradient-based approaches
  - Virtual experiments framework

[1] M. Pastorino, 'Stochastic optimization methods applied to microwave imaging: A review', *IEEE Trans. Antennas Propag.*, 2007.
[2] A. Randazzo, 'Swarm optimization methods in microwave imaging', ***Int. J. Microw. Sci. Tech.***, 2012.
[3] I. T. Rekanos, 'Shape reconstruction of a perfectly conducting scatterer using differential evolution and particle swarm optimization', ***IEEE Trans. Geosci. Remote Sens.***, 2008.
[4] A. Qing and C. K. Lee, Eds., ***Differential Evolution in Electromagnetics***, 2010.
[5] P. M. van den Berg and A. Abubakar, 'Contrast source inversion method: state of art', ***Prog. Electromag. Res.***, 2001.
[6] K. G. Brown, N. Geddert, M. Asefi, J. LoVetri, and I. Jeffrey, 'Hybridizable discontinuous galerkin method contrast source inversion of 2-d and 3-d dielectric and magnetic targets', ***IEEE Trans. Microw. Theory Techn.***, 2019.
[7] M. Ostadrahimi, P. Mojabi, A. Zakaria, J. LoVetri, and L. Shafai, 'Enhancement of Gauss-Newton inversion method for biological tissue imaging', ***IEEE Trans. Microw. Theory Techn.***, 2013.
[8] M. Salucci, G. Oliveri, A. Randazzo, M. Pastorino, and A. Massa, 'Electromagnetic subsurface prospecting by a fully nonlinear multifocusing inexact Newton method', ***J. Opt. Soc. Am. A***, 2014.
[9] M. T. Bevacqua, R. Palmeri, T. Isernia, and L. Crocco, 'A simple procedure to design virtual experiments for microwave inverse scattering', ***IEEE Trans. Antennas Propag.***, 2021.

An example of quantitative deterministic scheme

- To solve the nonlinear inverse-scattering problem, an inexact-Newton iterative method can be applied to minimize the residual functional $\Psi: X \to \mathbb{R}$

$$\Psi(x) = \frac{1}{2}\|\mathcal{F}(x) - y\|_Y^2 ,$$

  where $x \in X$, $y \in Y$, $F: X \to Y$, and $\|\cdot\|_Y$ denotes the norm of the functional space Y

- In constant exponent Lebesgue spaces, the the L^p-norm of a function u, for $1 \leq p < +\infty$, is defined as

$$\|u\|_{L^p}^p = \int |u(\mathbf{r})|^p d\mathbf{r}$$

- In the conventional solving schemes, $p = 2 \Longrightarrow X$ and Y are L^2 Hilbert space of square-integrable functions.

An example of quantitative deterministic scheme

- Inversion procedures in constant exponent Lebesgue spaces provide good results, but the main problem is the choice of the optimal p.
- To address this problem, a different class of Lebesgue spaces can be adopted – the variable exponent Lebesgue spaces $L^{p(\cdot)}$ – which allow setting different values of the parameter p inside the investigation domain.
- This is obtained by exploiting the Luxemburg norm, in which the power p is not constant, but it is a function $p(\cdot)$ of the domain, i.e.,

$$\|u\|_{L^{p(\cdot)}} = \inf\left\{\gamma > 0:\ \rho\left(\frac{u}{\gamma}\right) \leq 1\right\}$$

$$\text{Modulus: } \rho(u) = \int |u(\mathbf{r})|^{p(\mathbf{r})} d\mathbf{r}$$

An example of quantitative deterministic scheme

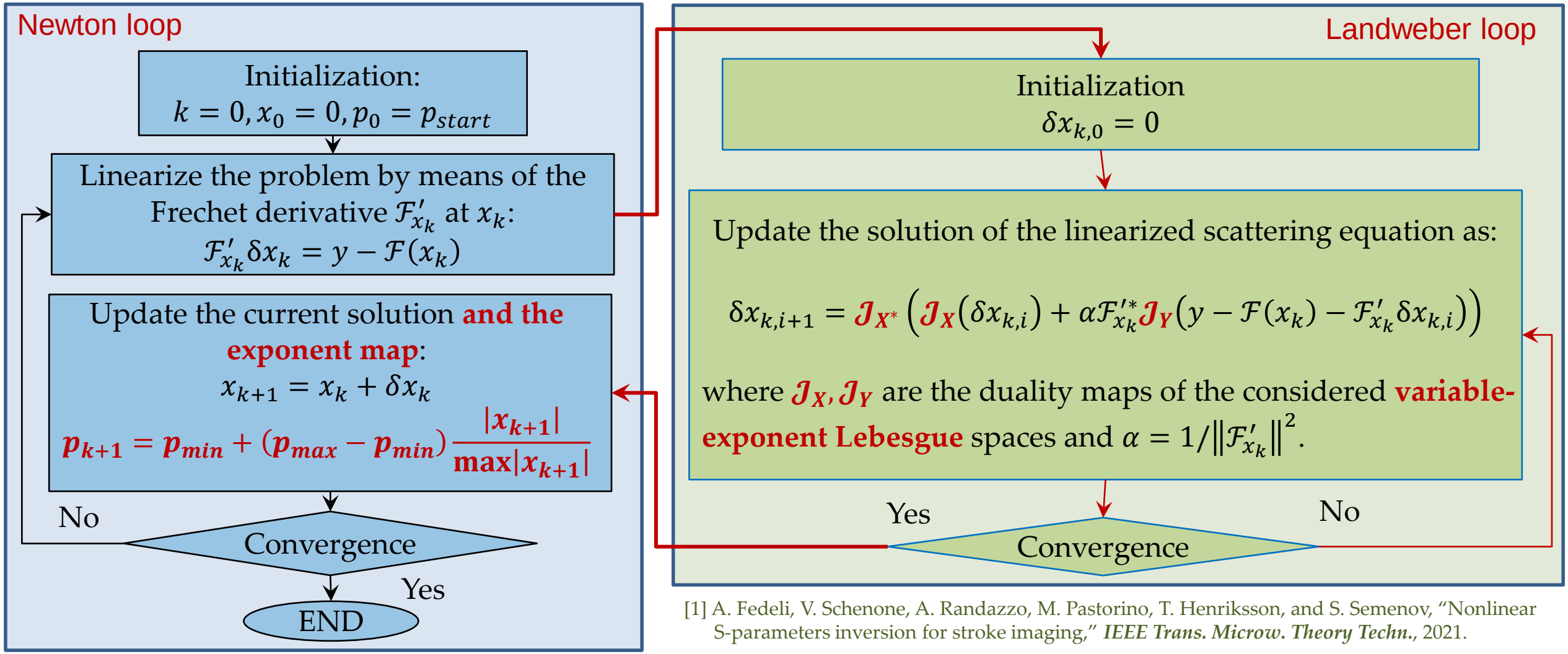

[1] A. Fedeli, V. Schenone, A. Randazzo, M. Pastorino, T. Henriksson, and S. Semenov, "Nonlinear S-parameters inversion for stroke imaging," *IEEE Trans. Microw. Theory Techn.*, 2021.

Applicative example – Wood tomography

- Developed in cooperation with SUPSI, Lugano (Switzerland) [1]
  - Multi-view/multi-illumination apparatus
  - Rotating platform hosting the SUT
  - Fiberglass supports for antennas vertical movement
  - Stepped motors for automatic measurements
  - Off-the-shelf VNA for stepped-frequency field generation/measurement
  - Multi-purpose system

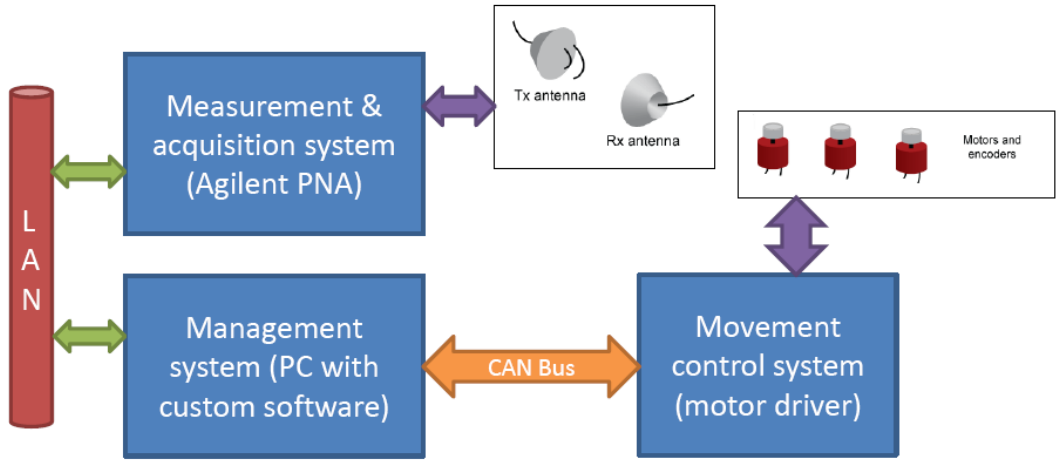

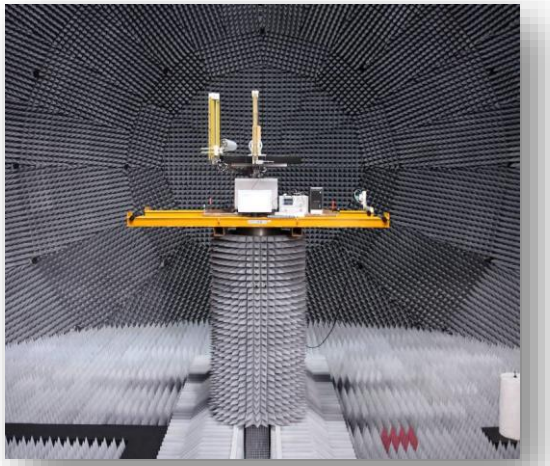

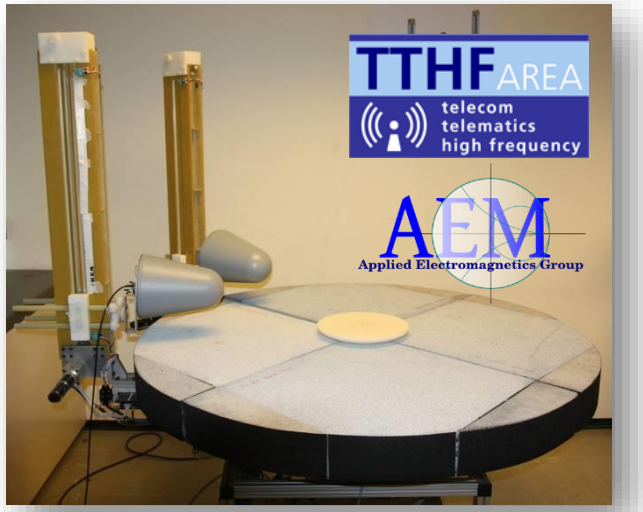

[1] A. Salvade, M. Pastorino, R. Monleone, G. Bozza, and A. Randazzo, "A New Microwave Axial Tomograph for the Inspection of Dielectric Materials," **IEEE Trans. Instrum. Meas.**, vol. 58, no. 7, pp. 2072–2079, Jul. 2009.

Applicative example – Wood tomography

- Two adjacent targets
  - Rectangular wood slab : sides lengths 11.5 cm and 7.5 cm, height 50 cm, center (0.3,8) cm, $\epsilon_r \approx 2.75$.
  - Rectangular hollow wood slab: sides lengths 11.5 cm and 7.5 cm, height 50 cm, center (0.3,8) cm, $\epsilon_r \approx 2.25$. A void hole (side lengths 5.5 cm and 3.5 cm) is present in the center of the slab.
- Measurement setup: $V = 16$ views, $M = 91$ measurement points per view on arc of circumference of 270 degrees.
- Frequency range: 1-6 GHz

Targets

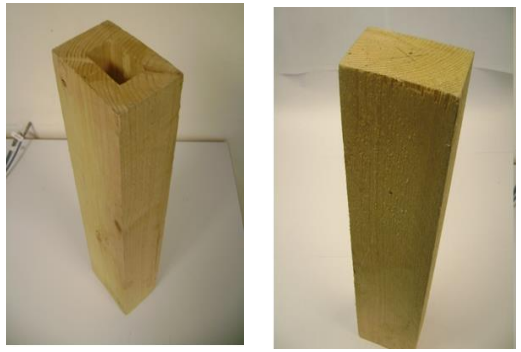

Mean relative errors vs norm parameter

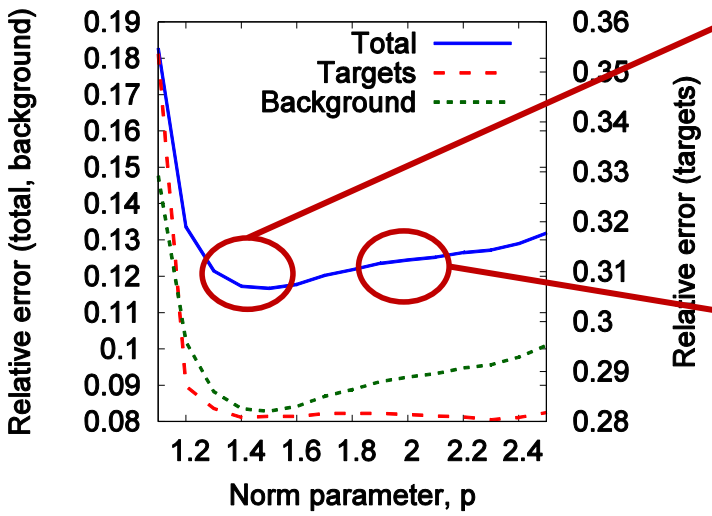

Reconstructed relative dielectric permittivity

Hollow wood slab

Wood slab.

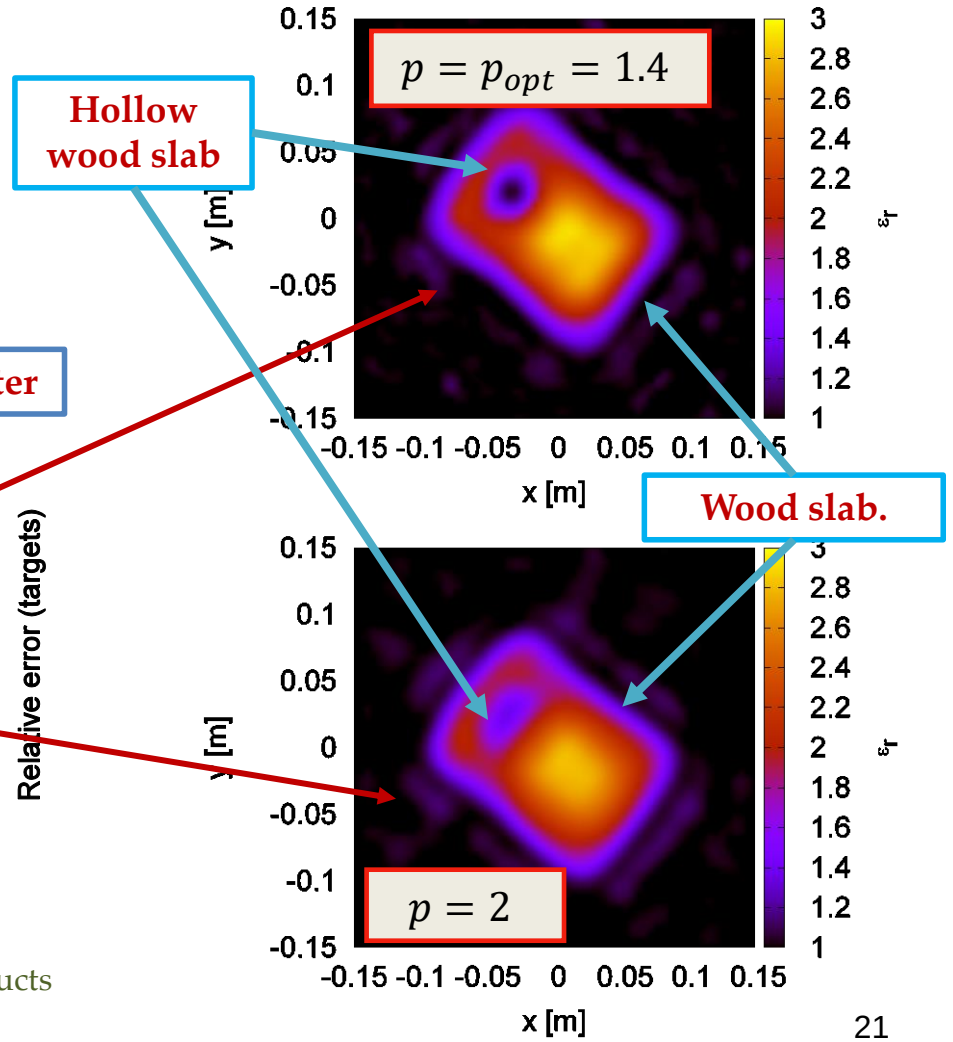

[1] M. Pastorino et al., "A microwave tomographic system for wood characterization in the forest products industry," **Wood Material Science and Engineering**, vol. 10, no. 1, pp. 75–85, 2015.

Hybrid qualitative/quantitative scheme [1]

- First step (time domain, synthetic pulse obtained with IFFT)
  - Incident pulse, air-sample & multiple layers scattering effects are removed by the filtering stage → estimation of the field scattered by the inclusion $\Delta\hat{e} = \Phi(e)$, where Φ is a proper filtering operator [2].
  - A qualitative image is produced by means of a delay-and-sum beamforming method [3].
- Second step (frequency domain)
  - A weighted inexact-Newton reconstruction exploits the information (scattered field and object location) obtained in the previous step to reconstruct maps of the dielectric properties.

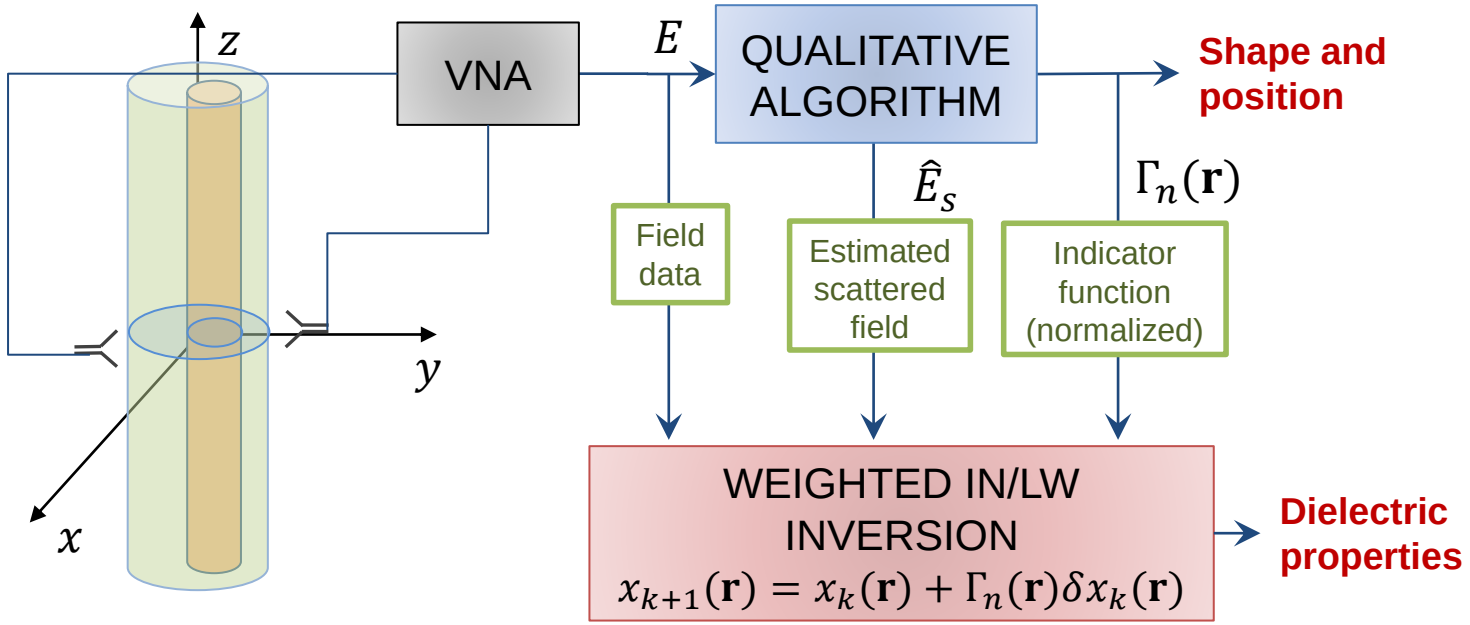

[1] F. Boero et al., "Microwave tomography for the inspection of wood materials: imaging system and experimental results," **IEEE Transactions on Microwave Theory and Techniques**, vol. 66, no. 7, pp. 3497–3510, Jul. 2018.

[2] E. J. Bond, X. Li, S. C. Hagness, and B. D. Van Veen, "Microwave imaging via space-time beamforming for early detection of breast cancer," **IEEE Trans. Antennas Propag.**, 2003.

[3] X. Li and S. C. Hagness, "A confocal microwave imaging algorithm for breast cancer detection," **IEEE Microw. Wirel. Compon. Lett.**, 2001.

Applicative example – Wood tomography

- Target configuration
  - Wood circular cylinder of diameter $d_c = 0.168$ m, height $h = 0.26$ m, dielectric permittivity $\epsilon_r \simeq 6$ and electric conductivity $\sigma \simeq 0.06$ S/m
  - Void Square hole with diagonal $d_i = 0.06$ m
  - Investigation domain partitioned into $N = 708$ square cells of side $l = 0.0056$ m (External shape estimated from antenna positions).
- Measurement configuration
  - Antennas in contact with the target
  - $V = 32$ views with $V - 1$ meas. pts.
  - $F = 64$ frequency steps between 400 MHz and 1.4 GHz
- Algorithm parameters
  - IN/LW residual var. thr. 1%.
  - 10 max outer/inner iterations

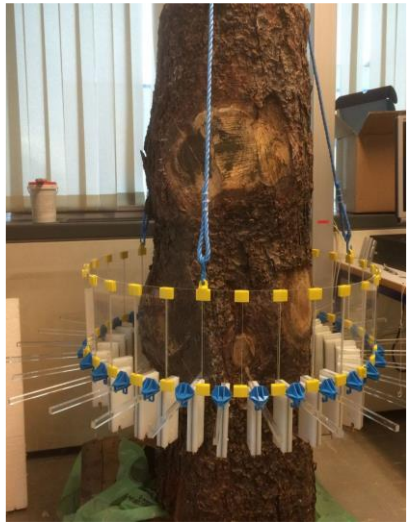

Actual target image

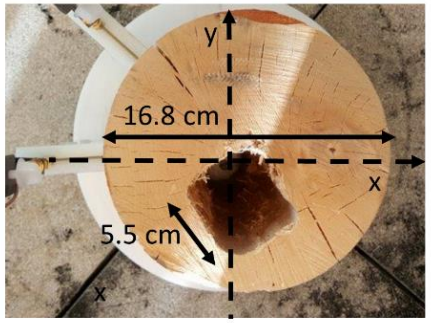

Qualitative indicator map

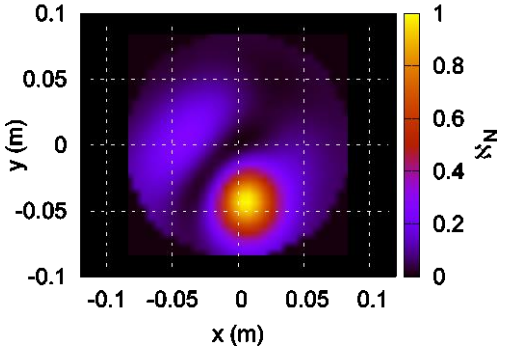

Relative dielectric permittivity

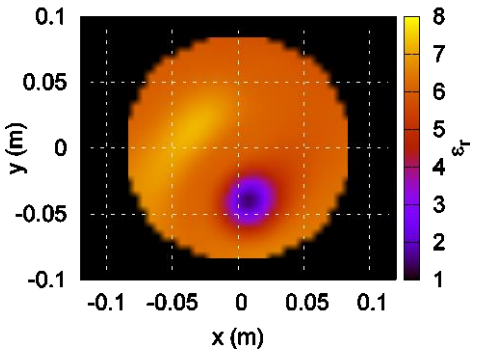

Electric conductivity

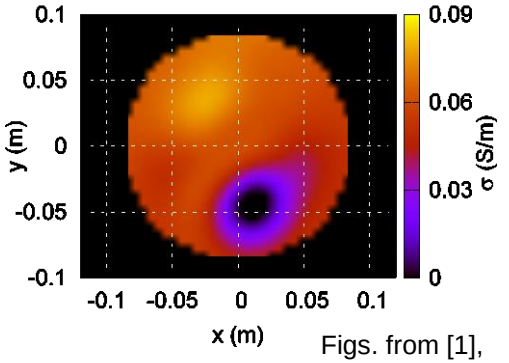

Figs. from [1], reproduced with permission.

[1] F. Boero et al., "Microwave tomography for the inspection of wood materials: imaging system and experimental results," **IEEE Transactions on Microwave Theory and Techniques**, vol. 66, no. 7, pp. 3497–3510, Jul. 2018.

Applicative example – Buried object detection

- Measurement configuration
  - Quasi-monostatic GPR arrangement
  - Constant TX/RX offset ΔL are moved along the probing line over the soil surface

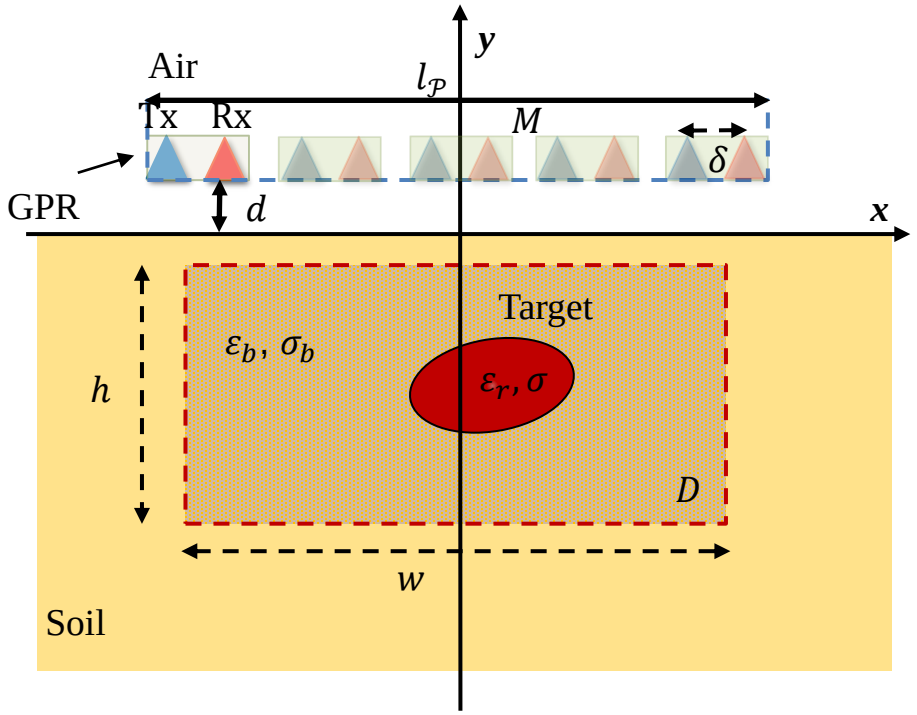

Measurement parameters

GPR offset	$\Delta L = 20$ cm
Height of measurement line	$d = 1$ cm
Length of measurement line	$l = 2$ m
GPR scans step	$\Delta R = 2$ cm

Soil parameters

Background permittivity	$\epsilon_b \simeq 5\,\epsilon_0$
Background el. conductivity	$\sigma_b \simeq 38 \times 10^{-3}$ S/m

Targets

[1]"NSGG UXO Test Site," Geomatrix Earth Science Limited. https://www.geomatrix.co.uk/tools/nsgg-uxo-test-site/ - Photos courtesy of Matt Guy.

Applicative example – Buried object detection

Initial choice of exponent map:

$$p_0(\mathbf{r}) = p_{min} + (p_{max} - p_{min})\Gamma_n(\mathbf{r})$$

- **NSGG experimental dataset**
- Investigation domain
  ($L = 0.8$ m, $W = 1$ m,
  $\mathbf{r}_{t,\mathcal{D}} = (0, -0.45)$ m)
- Frequency band:
  B = [150 − 400] MHz
- $F = 4$ considered frequencies in B and a subset of six equally spaced receiver positions
- Method parameters:
  $I_{LW} = 10$, $K_{IN} = 20$, $p_{min} = 1.5$, $p_{max} = 2.0$ Res. var. thr. 0.1

Reconstructed qualitative map

Reconstructed relative dielectric permittivity by the pure quantitative method

Reconstructed relative dielectric permittivity by the hybrid inversion method

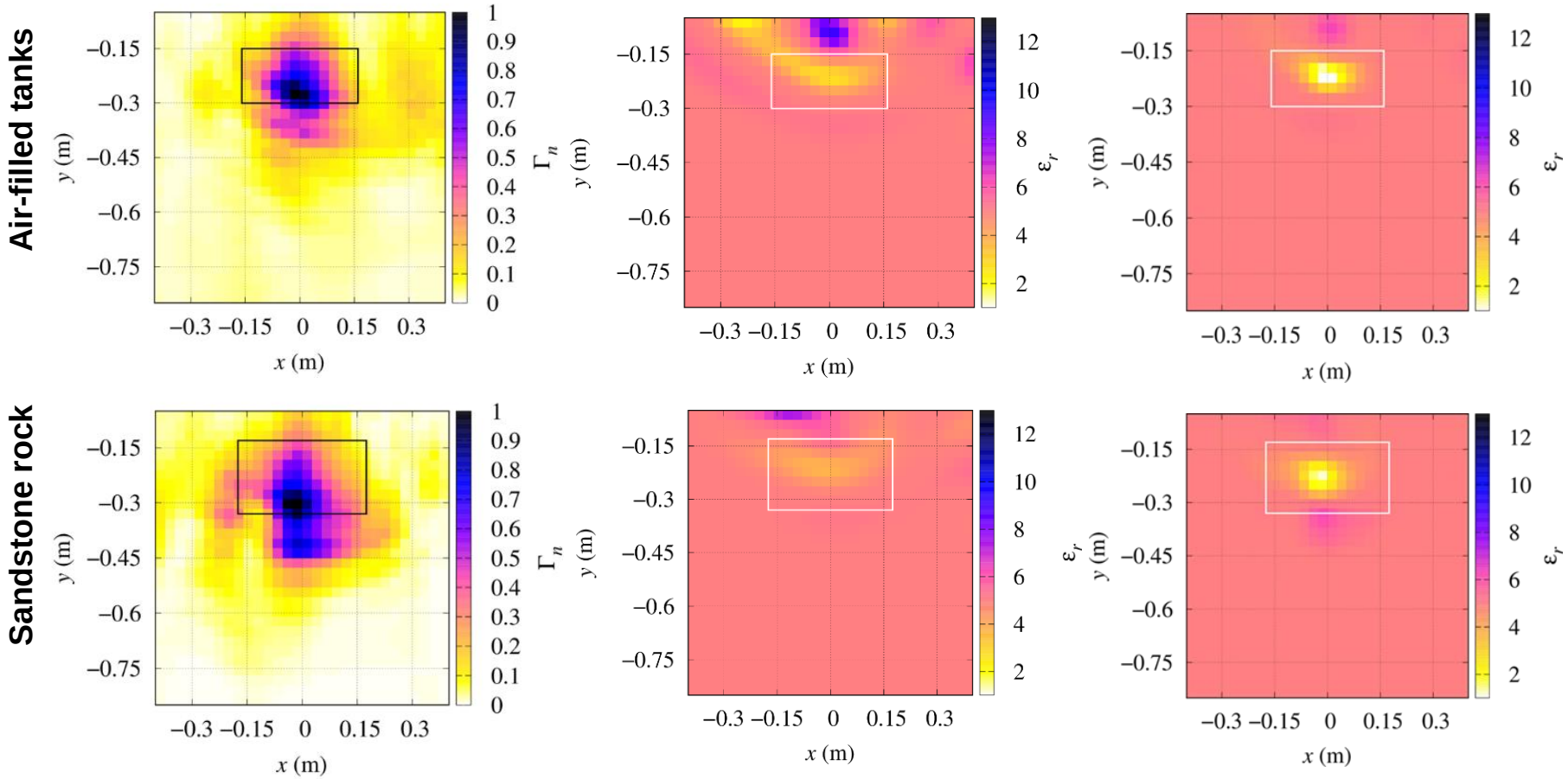

[1] V. Schenone, A. Fedeli, C. Estatico, M. Pastorino, and A. Randazzo, 'Experimental Assessment of a Novel Hybrid Scheme for Quantitative GPR Imaging', **IEEE Geoscience and Remote Sensing Letters**, vol. 19, pp. 1–5, 2022.

Figs. from [1], reproduced with permission.

An applicative example – Brain stroke detection and monitoring

- Brain stroke is well known as one of the leading causes of death and disability worldwide
  - Ischemic → ischemia due to the obstruction of blood vessels
  - Hemorrhagic → hemorrhage due to the rupture of blood vessels
- **Similar** symptoms, but **radically different** therapies!

Actual therapies should be administered in the first hours from the occurrence of symptoms → **Early diagnosis**!

- CT and MRI provide good diagnostic images, but can be used only at the hospital
- Portable systems, that can be used in the ambulance, are desirable!
- Several microwave-based techniques and system prototypes are currently under development [1]

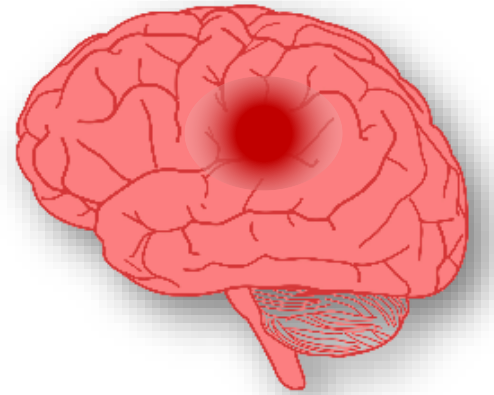

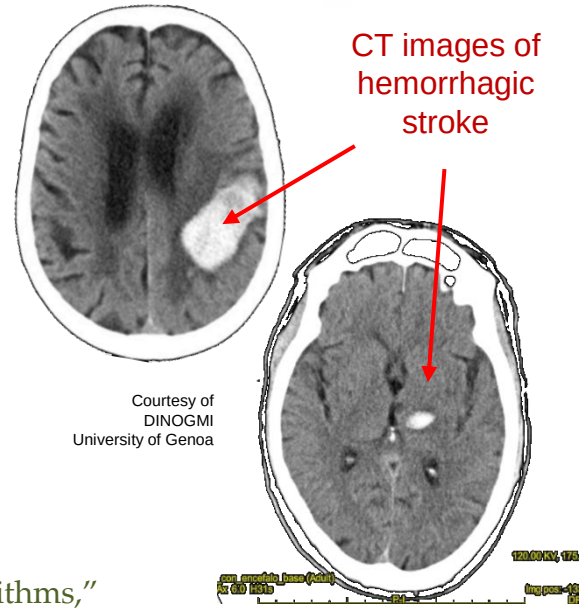

[1] L. Guo, A. S. M. Alqadami, and A. Abbosh, "Stroke diagnosis using microwave techniques: Review of systems and algorithms," *IEEE Journal of Electromagnetics, RF and Microwaves in Medicine and Biology*, vol. 7, no. 2, pp. 122–135, Jun. 2023.

An applicative example – Brain stroke detection and monitoring

- Experimental validation with a prototype of stroke monitoring system [1][2] and a simplified cylindrical head phatom.
- Multistatic measurement setup with $S = 16$ antennas and working in the band [500,900] MHz.
- Coupling medium (70% glycerin/water mixture) between antennas and target (PE bags).
- Target properties:
  - Outer structure: polypropylene beaker (D=180 mm) filled with 70% glycerin/water mixture
  - Cylindrical inclusions: polypropylene circular cylinders (D=20 mm and D=52 mm) filled with 0.9% saline solution.

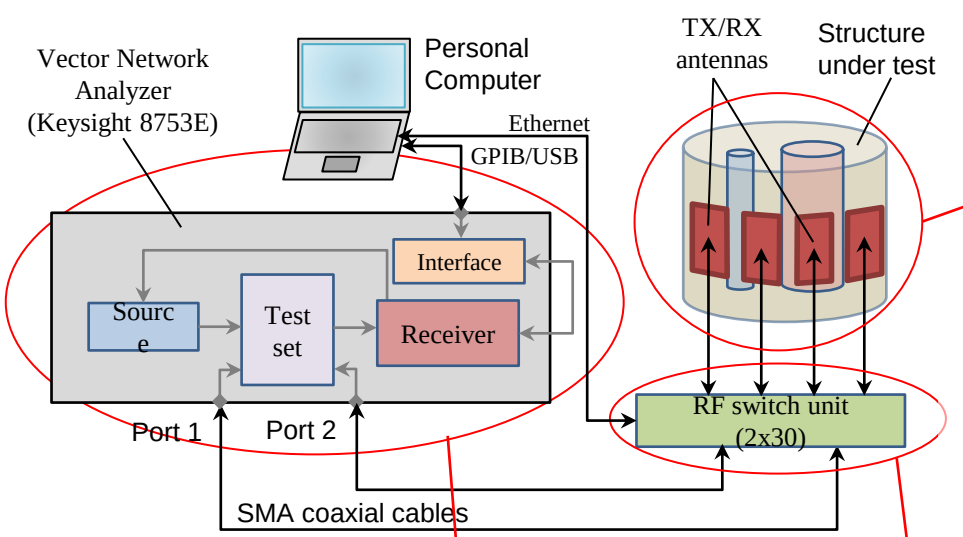

Measurement setup

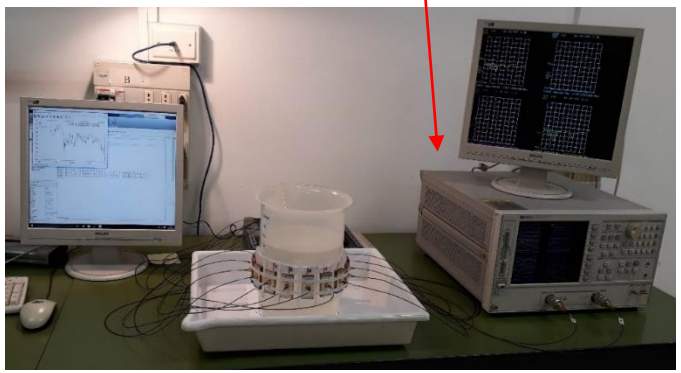

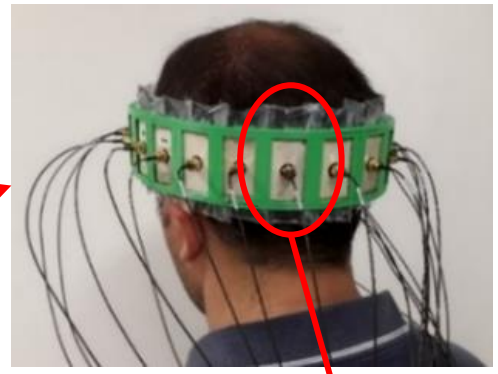

16 cavity-backed antennas with slotted bowtie-like structure

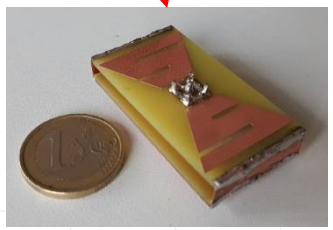

RF switch unit

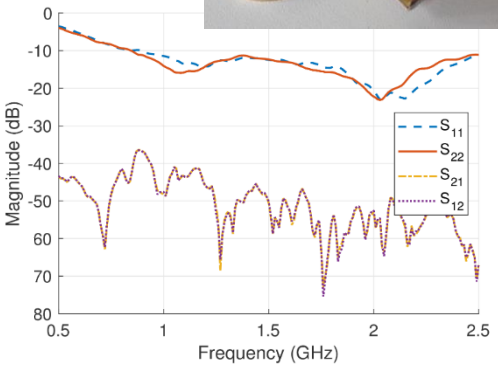

Measured scattering parameters

[1] I. Bisio et al., 'Brain stroke microwave imaging by means of a Newton-conjugate-gradient method in L^p Banach spaces,' **IEEE Trans. Microw. Theory Techn.**, 2018.
[2] I. Bisio et al., 'Variable-exponent Lebesgue-space inversion for brain stroke microwave imaging', ***IEEE Trans. Microw. Theory Techn.***, 2020.

Figs. from [1], reproduced with permission.

An applicative example – Brain stroke detection and monitoring

Target configuration – Single circular inclusion

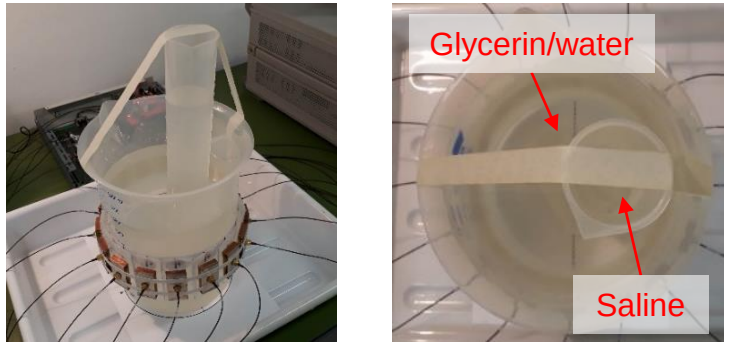

Reconstructed relative dielectric properties (variable exponent)

f=600 MHz

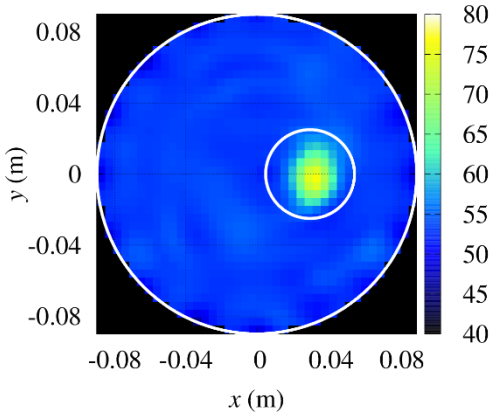

f=900 MHz

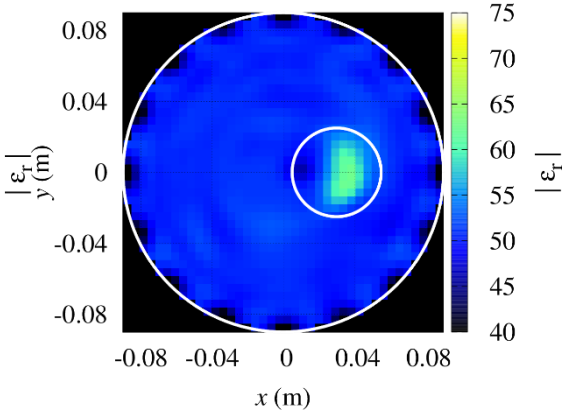

Target configuration – Two circular inclusions with different size

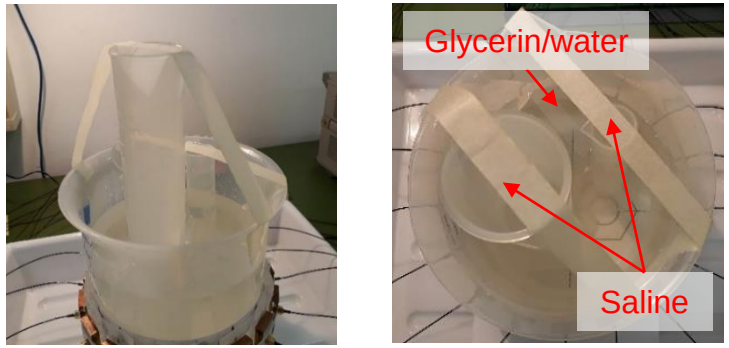

Reconstructed relative dielectric properties (variable exponent)

f=600 MHz

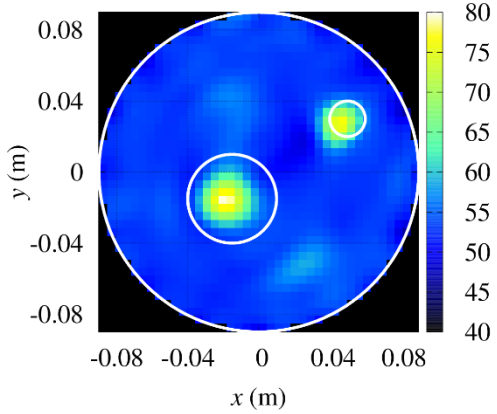

f=900 MHz

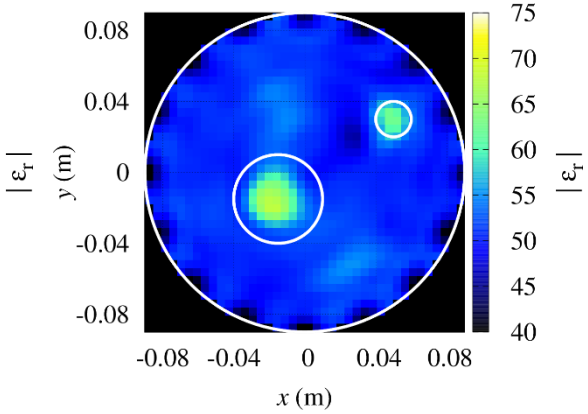

[1] I. Bisio et al., 'Variable-exponent Lebesgue-space inversion for brain stroke microwave imaging,' **IEEE Trans. Microw. Theory Techn.**, 2020.

Figs. from [1], reproduced with permission.

An applicative example – Brain stroke detection and monitoring

- An example of brain stroke imaging system based on a metallic chamber: The EMTensor brain scanner
- Target: SAM phantom filled with a glycerin/water mixture ($\epsilon_b = (46.5 - j18.8)\epsilon_0$) containing a ellipsoidal inclusion simulating a hemorrhaging stroke.
- Inversion parameters: 50 max inner/outer iterations; norm. residual var. thr., 0.1%, reference configuration: empty chamber

Experimental system

Head phantom

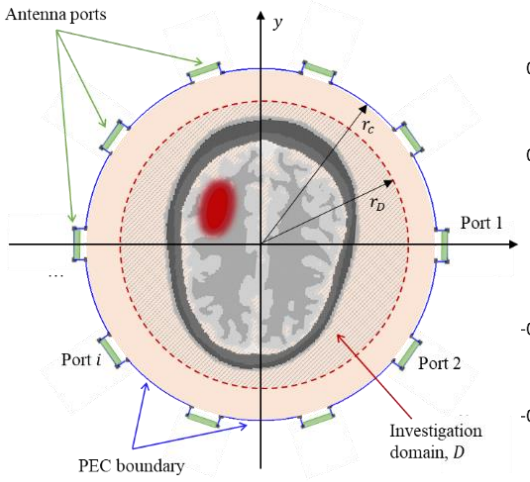

ϵ_r (real part)

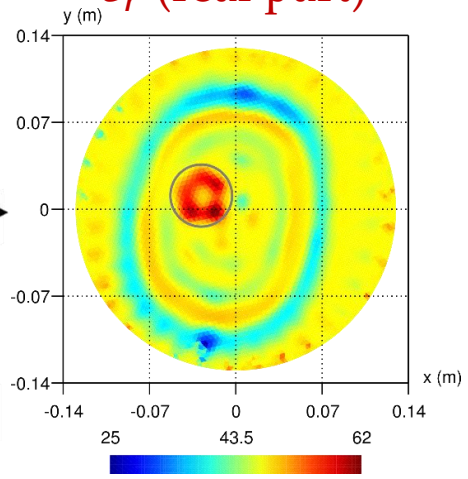

ϵ_r (imaginary part)

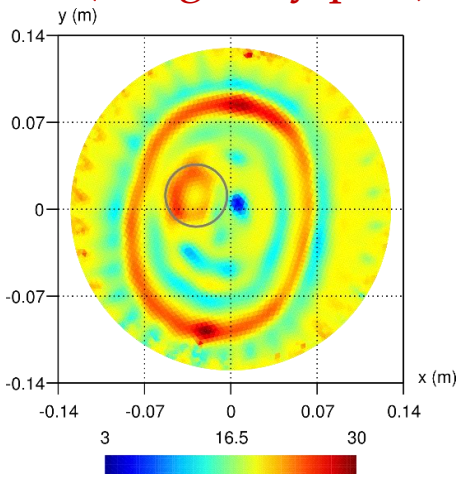

Figs. from [1], reproduced with permission.

Number of antennas	192 (6 rings of 32)
Number of transceiver units	192
Tx power	0 dBm
Rx sensitivity	>-140 dBm
Frequency band	0.92-1.08 GHz
Data acquisition time	0.16-5s
Total size (H / W / D)	135 x 120 x 78 cm
Power consumption	<1.8 kW

[1] A. Fedeli, V. Schenone, A. Randazzo, M. Pastorino, T. Henriksson, and S. Semenov, 'Nonlinear S-parameters inversion for stroke imaging', *IEEE Trans. Microw. Theory Techn.*, 2021.

Modern ML techniques applied to microwave imaging

- More recently, thanks to the increased computational power, approaches based on deep neural networks have been devised, too.

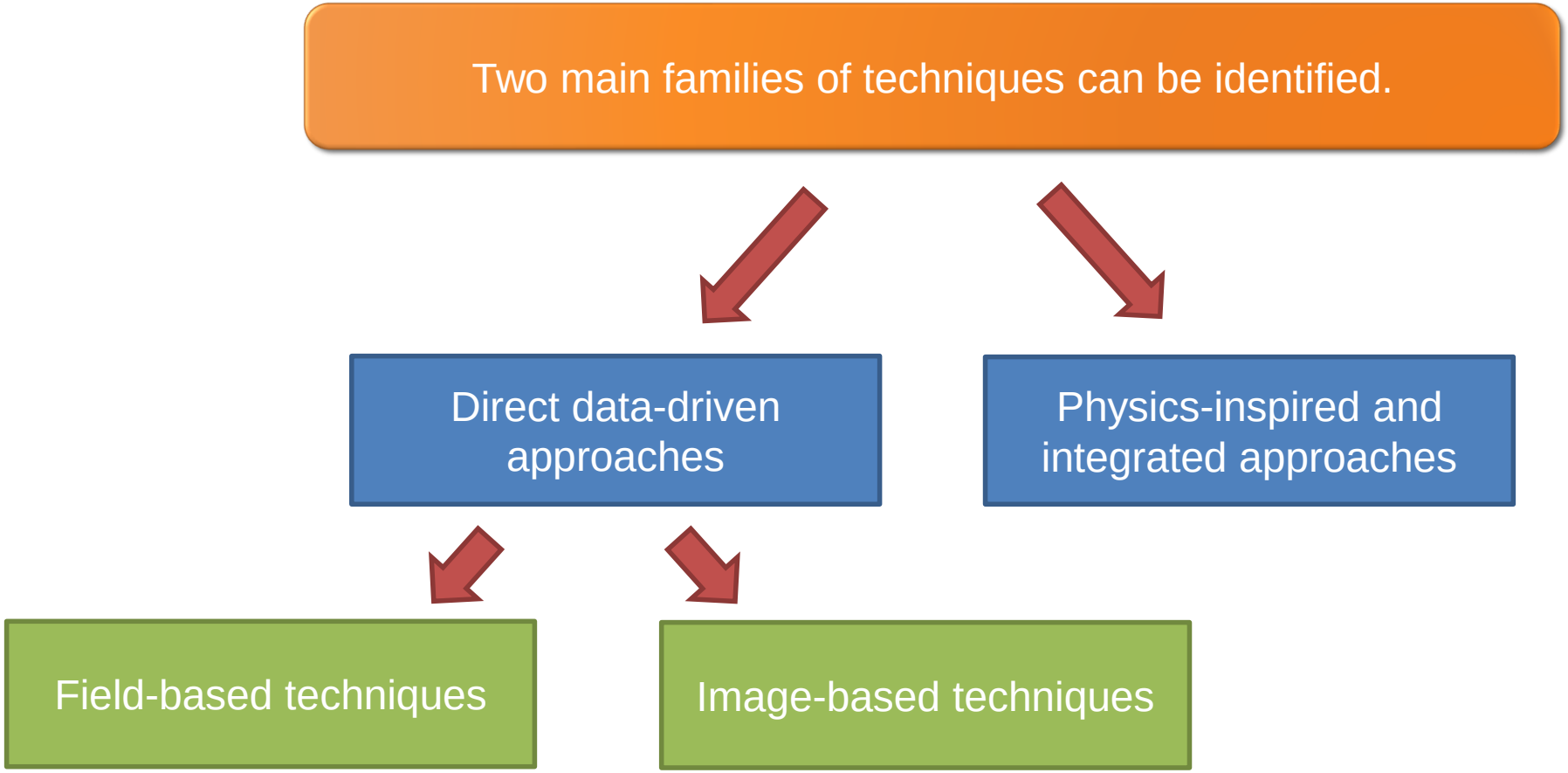

Modern ML techniques applied to microwave imaging

- In direct data-driven approaches, the map connecting the measurements (eventually pre-processed) and the distributions of dielectric properties are modeled through a deep network → Two main classes:
  1) Neural networks are trained to directly learn the mapping between the scattered electric fields and the dielectric property images.
     - C. Dachena, A. Fedeli, A. Fanti, M. B. Lodi, G. Fumera, A. Randazzo, and M. Pastorino, "Microwave Imaging of the Neck by Means of Artificial Neural Networks for Tumor Detection," ***IEEE Open J. Antennas Propag.***, 2021.
     - J. Wang, H. Liu, P. Jiang, Z. Wang, Q. Sui, and F. Zhang, "GPRI2Net: A Deep-Neural-Network-Based Ground Penetrating Radar Data Inversion and Object Identification Framework for Consecutive and Long Survey Lines," ***IEEE Trans. Geosci. Remote Sens.***, 2022.
  2) A conventional technique is used to create an initial reconstruction, which is then enhanced using neural networks
     - V. Khoshdel, M. Asefi, A. Ashraf, and J. LoVetri, "Full 3D Microwave Breast Imaging Using a Deep-Learning Technique," ***J. Imag.***, 2020.

- In physics-based approaches, a òink between the physics of the inverse problem and the learning scheme is exploited, e.g.,
  - Z. Wei and X. Chen, "Physics-Inspired Convolutional Neural Network for Solving Full-Wave Inverse Scattering Problems," ***IEEE Trans. Antennas Propag.***, 2019.
  - M. Li et al., "Machine learning in electromagnetics with applications to biomedical imaging: a review," ***IEEE Antennas and Propagation Magazine***, vol. 63, no. 3, pp. 39–51, Jun. 2021.

An applicative example — Neck imaging

- Microwave imaging may be potentially suitable for the identification of some neck pathologies, e.g.,
  - Larynx tumors
  - Cervical myelopathy
- Fully-connected architecture with H hidden layers and D neurons for each layer ($H = 5$, $D = 448$) [1]
- The ADAM method is adopted in the training phase:
  - D=30,000 configurations with random geometrical and dielectric properties; training: 95% of data; validation: 5% of data
  - Random initial weights w/ Gaussian distribution
  - L^2 regularization term with parameter set to 10^{-4}

Loss function

$$\mathcal{L} = \sum \frac{\left\| \varepsilon_{r,rec} - \varepsilon_{r,real} \right\|^2}{\left\| \varepsilon_{r,real} \right\|^2} + \sum \frac{\left\| \sigma_{rec} - \sigma_{real} \right\|^2}{\left\| \sigma_{real} \right\|^2}$$

Larynx Tumor (CT scan)

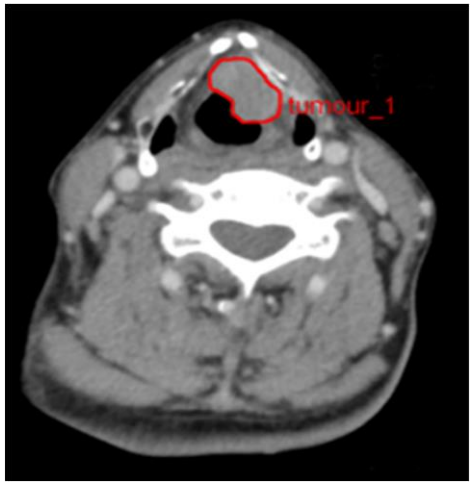

Cervical Myelopathy (MRI scan)

Training model

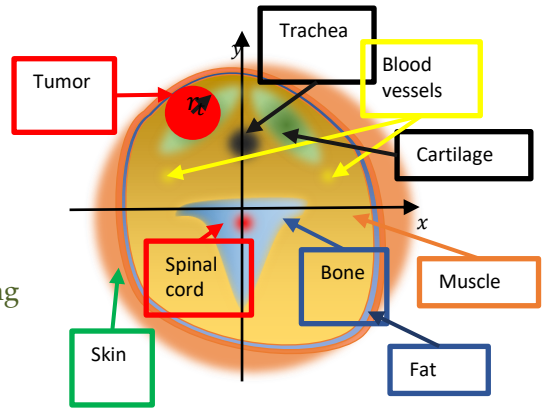

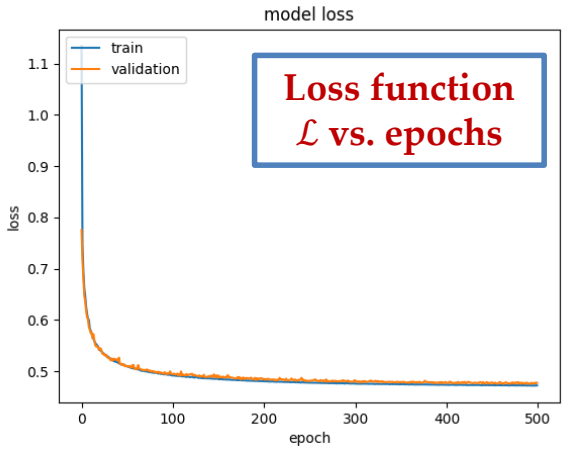

Loss function $\mathcal{L}$ vs. epochs

[1] C. Dachena, A. Fedeli, A. Fanti, M. B. Lodi, M. Pastorino, and A. Randazzo, 'Microwave imaging for the diagnosis of cervical diseases: A feasibility analysis', ***IEEE J. Electromag. RF Microw. Med. Biol.***, 2021.

[2] C. Dachena, A. Fedeli, A. Fanti, M. B. Lodi, G. Fumera, A. Randazzo, and M. Pastorino, "Microwave Imaging of the Neck by Means of Artificial Neural Networks for Tumor Detection," ***IEEE Open J. Antennas Propag.***, 2021.

An applicative example — Neck imaging

- Imaging configuration:
  - $N = 10$ TX/RX ideal antennas
  - $F = 7$ frequencies in the range [600–900] MHz
  - Investigation domain: $N_s = 5024$ square cells of 2 mm side
- Simulated scattered-field data corrupted with Gaussian noise with $SNR = 35\ dB$

Distributions of reconstructed dielectric properties

Tumor radius $r_t = 15$ mm

Relative dielectric permittivity

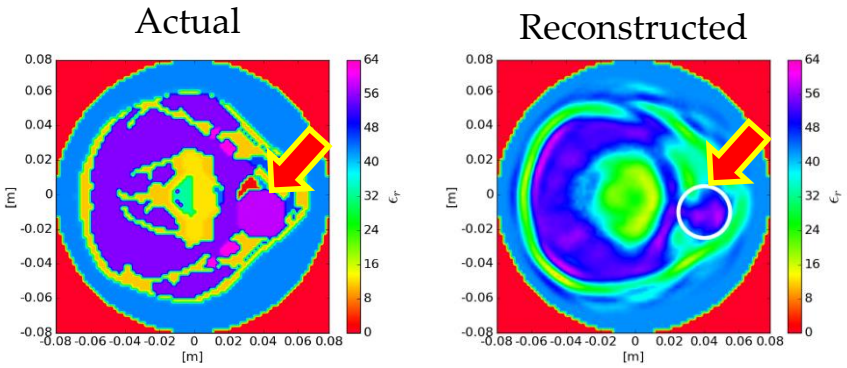

Electric conductivity

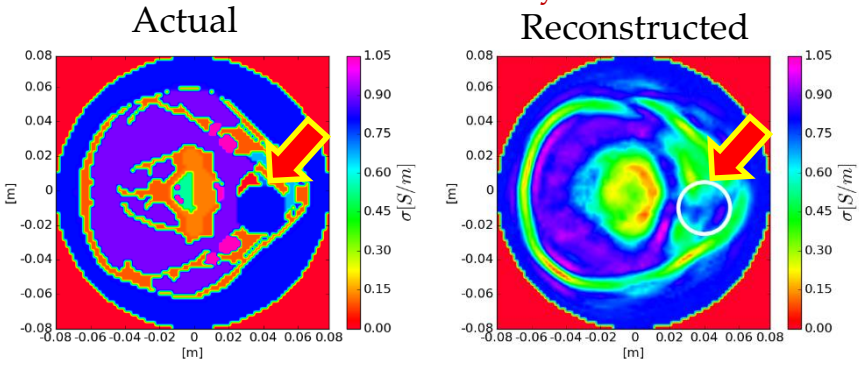

Tumor radius $r_t = 10$ mm

Relative dielectric permittivity

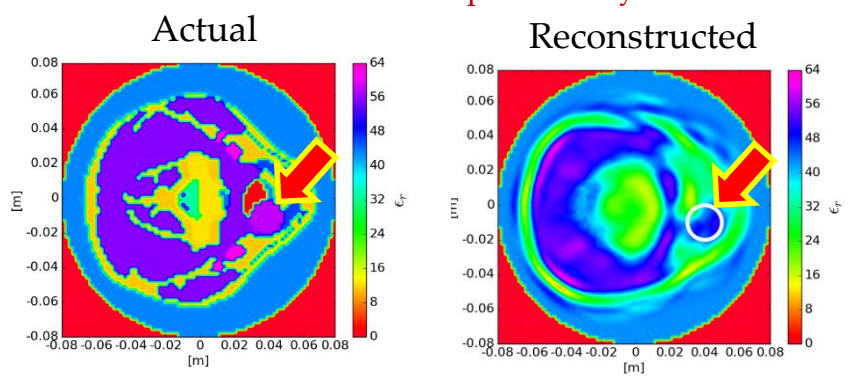

Electric conductivity

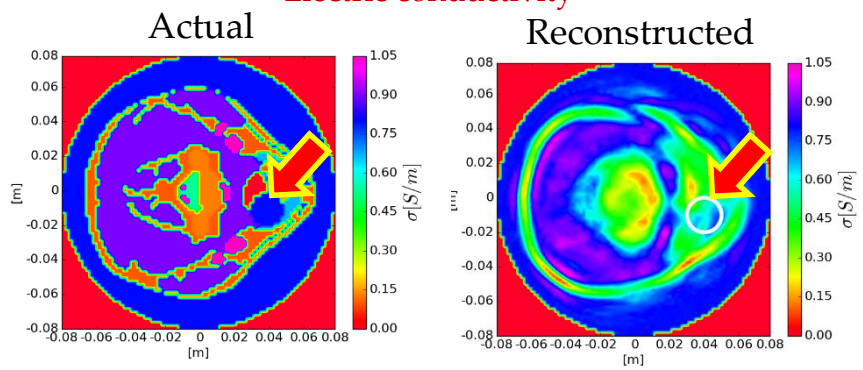

[1] C. Dachena, A. Fedeli, A. Fanti, M. B. Lodi, G. Fumera, A. Randazzo, and M. Pastorino, "Microwave Imaging of the Neck by Means of Artificial Neural Networks for Tumor Detection," *IEEE Open J. Antennas Propag.*, 2021.

An applicative example — Neck imaging

Glass beaker phantom

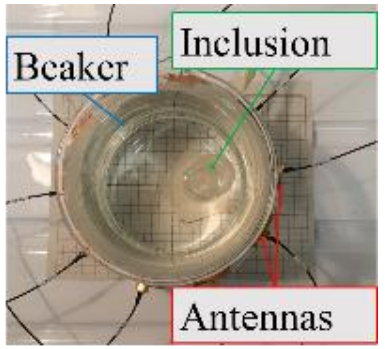

3D printed neck phantom with one cylindrical inclusion

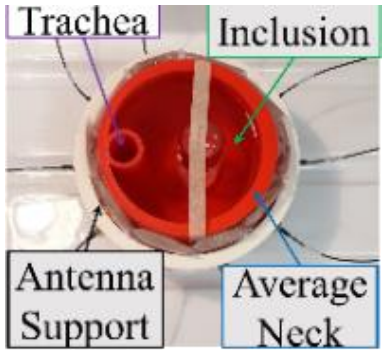

3D printed phantom with simplified model of vertebral column

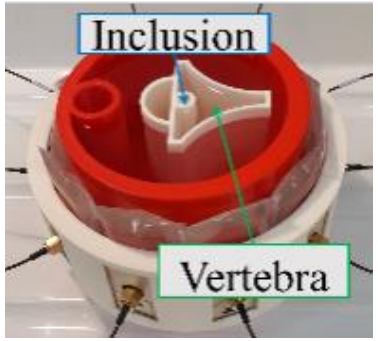

Differential relative dielectric permittivity

Differential electric conductivity

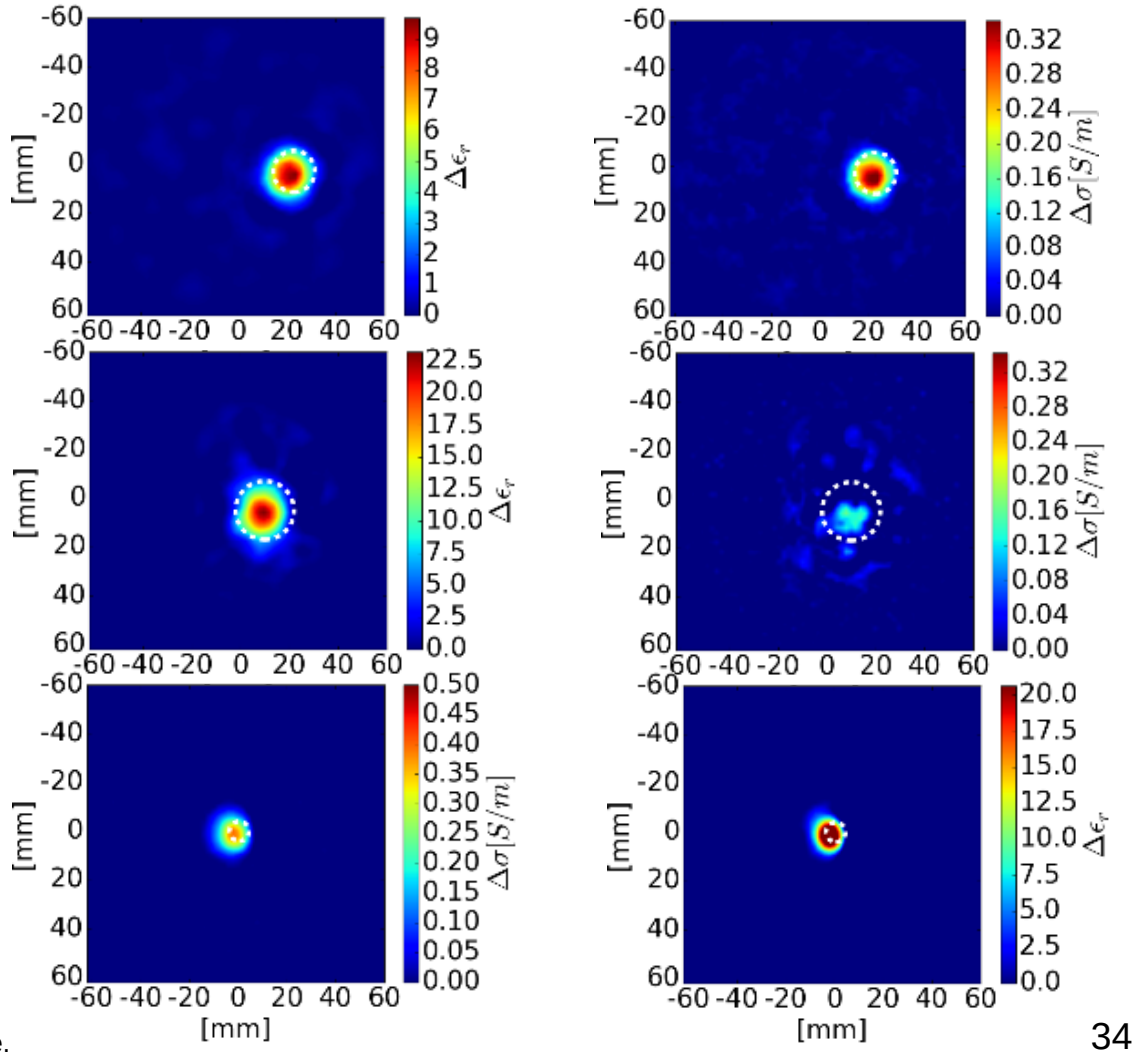

[1] C. Dachena et al., "Initial Experimental Tests of an ANN-Based Microwave Imaging Technique for Neck Diagnostics," *IEEE Microwave and Wireless Components Letters*, vol. 32, no. 12, pp. 1495–1498, Dec. 2022.

Conclusions and future perspectives

- Microwave imaging
  - A technique aimed at inspecting (non-destructively) targets starting from measurements of the electromagnetic field they scatter when illuminated by an incident radiation at microwave frequencies
  - A wide and ever-growing research field on which research activities of Prof. Matteo Pastorino were mainly focused

- New advancements, both in terms of systems and methods, are continuously proposed by the scientific community, bridging the gap between theory and practical applications.

- Microwave imaging is becoming a **competitive tool** in several fields
  - Industrial settings
  - Civil engineering
  - Subsurface prospecting
  - Medical diagnostics

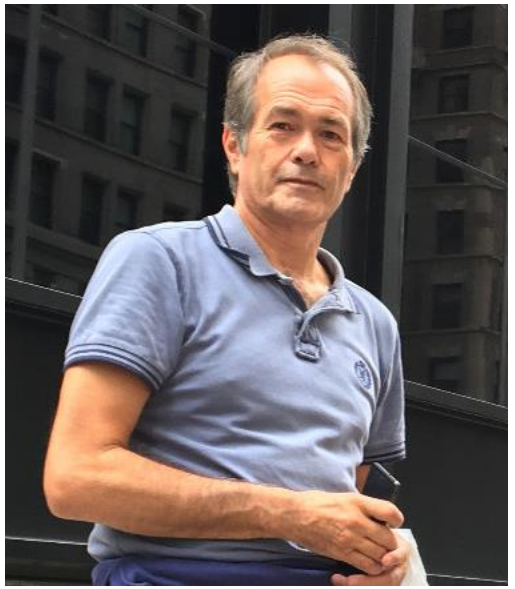

DITEN

2023 Italian National URSI meeting
November 17, 2023
Genova

Microwave imaging techniques and applications
(in memory of Matteo Pastorino)

Andrea Randazzo and Alessandro Fedeli

Many thanks for your attention!